Vol. 13(1): 60-74, January 2025 DOI: https://doi.org/10.23960/jsl.v13i1.1033

Jurnal Sylva Lestari

P-ISSN: 2339-0913
E-ISSN: 2549-5747

Journal homepage: https://sylvalestari.fp.unila.ac.id

Full Length Research Article

Disease Spectral Identification and Analysis on the Bark of Gmelina (*Gmelina arborea* Roxb)

Annie Onez Ayag[1], Kyra Luminarias Padonat[1], Kizza Eyn Sulima Minguita[1], Joey Arles Ongue Vergara[2,3], Jade Capinpuyan Jusoy[2,3], Cornelio Sacquiap Casilac Jr[1,*]

[1] College of Forestry and Environmental Science, Forestry Department, Caraga State University, Butuan, Philippines
[2] College of Mathematics and Natural Sciences, Department of Physics, Caraga State University, Butuan, Philippines
[3] Center for Nanoscience and Technology for Research Entrepreneurship, Caraga State University, Butuan, Philippines
[*] Corresponding Author. E-mail Address: corneliocasilac@gmail.com

ARTICLE HISTORY:

Received: 26 July 2024
Peer review completed: 17 December 2024
Received in revised form: 28 December 2024
Accepted: 7 January 2024

KEYWORDS:

Disease identification
Healthy bark
Gmelina arborea
Unhealthy bark
UV-Vis spectrometry

ABSTRACT

Gmelina arborea is among the fast-growing Industrial tree plantation species currently being used as an alternative source of the decreasing supply of commercial timber from natural-growth forests. This study focuses on disease spectral identification and analysis of *G. arborea* bark using UV-Vis Spectrophotometry. Bark samples from both healthy and unhealthy bark with canker and death diseases were collected inside Caraga State University's Main Campus. The methodology involved preparing bark extracts and measuring their absorbance over a wavelength range of 350 nm to 800 nm. The findings revealed distinct spectral signatures of healthy and unhealthy cankers, particularly with death disease, which exhibits a greater alteration in its spectral trend. The spectral trend of death-disease shows a drastic decrease in its absorption and the presence of troughs and peaks. On the other hand, the canker shows a decrease in its absorption. The severity of disease in the bark may potentially affect the behavior of the spectral trend; this is proven in the spectral trend of death-disease. The absorbance decreased, causing troughs at specific wavelengths as the presence of those diseases and their severity progressed. These findings show that spectral information from healthy and unhealthy bark can be used as an early detection method for tree diseases or stresses, thereby contributing to the conservation and sustainable use of *G. arborea*.

1. Introduction

Trees are among the most significant resources and raw materials in our economy, providing various economically important products (Aisyah et al. 2023; Hariz et al. 2023). However, trees are susceptible to infection due to external variables that impair their physiological processes, disrupting structure, development, and function (Nazarov et al. 2020). The condition's symptoms may vary depending on the cause, type, and location of the impact site.

In the Philippines, among the timber of high economic value is the Yemane (*Gmelina arborea* Roxb*)* is a fast-growing tree that can grow to be 30 m tall with a girth of 1.2 to 4 m (Sakthivel et al. 2017). Gmelina is a significant and highly valued species in the Philippines due

to its economic relevance (Vallesteros 2015). It accounts for most of the local wood supply volume, about 70% (FMB 2013). In neighboring countries like Indonesia, plantation forests supply about 85% of timber production logs (Aisyah et al. 2021). Besides the species being economically important, *G. arborea* is also susceptible to several diseases, causing several challenges for the tree (Anuagasi et al. 2017). The study of Belezaca-Pinargote et al. (2021) investigates the role of *Fusarium* spp. in the pathogenesis of Gmelina. The presence of and pathogenicity of the fungi Ceratocystis fimbriata causes the disease of the Gmelina tree (Macías-Moncayo 2019). These diseases stunt the growth of a tree, restricting its girth and height growth, hence decreasing the tree's commercial value. To advance in modern pest and disease management, the automatic identification of tree disease is crucial, and there are many approaches to plant disease identification and detection (Martinelli 2014). In the study of Martinelli et al. (2014), there are numerous reasons why there is a need to estimate or evaluate plant disease. Tree disease is correlated to productivity loss, so gaining a thorough understanding of disease management is vital. In practical use, specialists' primary method for detecting and identifying diseases is direct visual inspection, which may be excessively costly and time-consuming. Generally, the traditional approaches to diagnosing diseases first involve interpreting visual symptoms and laboratory assessment (Alemu 2015). Nowadays, there are numerous methods of plant disease identification, including a combination of spectroscopy-based methodologies. The UV-Vis spectroscopy, along with other optical techniques, offers rapid and non-invasive analysis across various plant parts and pathogens (Gudkov et al. 2023)

According to several studies, many spectroscopy approaches have recently been designed, developed, and applied as useful and practical tools for large-scale real-time plant disease diagnosis in the field (Abu-Khalaf and Salman 2014; Farber et al. 2019; Liaghat et al. 2014). Today, several methods, ranging from conventional to advanced techniques, have been used in the initial detection of plant disease (Sankaran et al. 2010).

In the study by Wei et al. (2021), UV-Vis spectrophotometry was used to provide graphical information on the spectral signature of healthy and unhealthy bark of *G. arborea*; it serves as an instrument to evaluate the distinctive patterns of the wavelength and frequency of both healthy and unhealthy tree bark samples that are affected by environmental factors and specific diseases associated by *G. arborea.* Since there are no formal studies on the effects of specific diseases on the behavior of the wavelengths of the bark of *G. arborea* tree using UV-Vis spectrophotometry and how it differs from a healthy bark, research priority includes developing an understanding of the substantial differences in its wavelength behavior acquired from spectral analysis.

2. Materials and Methods

2.1. Location of the Study

This study was conducted at Caraga State University-Main Campus Barangay Ampayon, Butuan City, Agusan del Norte, as shown in **Fig. 1**. The area has no definite dry season. Rainfall is pronounced throughout the year, with maximum rainfall from November to January. It demonstrates the location of healthy and diseased bark of *G. arborea* afflicted by canker and death-disease that have been selectively chosen as sources for sample collection in this study. Thus, providing a comprehensive spatial overview is crucial to understanding the health dynamics of this tree species on campus.

2.2. Data Gathering

Six (6) *G. arborea* trees were randomly selected to be extracted with bark samples at Caraga State University based on the diameter at breast height (DBH) of the tree and tree height (TH). The tree sample diameter at breast height ranges from 20–40 cm DBH. The basis for the selection of tree samples was based upon previous research by Hadlich et al. (2018) and Sandak et al. (2016), where tree samples DBH ranges from ≥ 10 cm, the collection of bark samples was done between the 2 m or so in a standing tree which is readily available for sampling to reduce radial variation from pith to bark (**Table 1**).

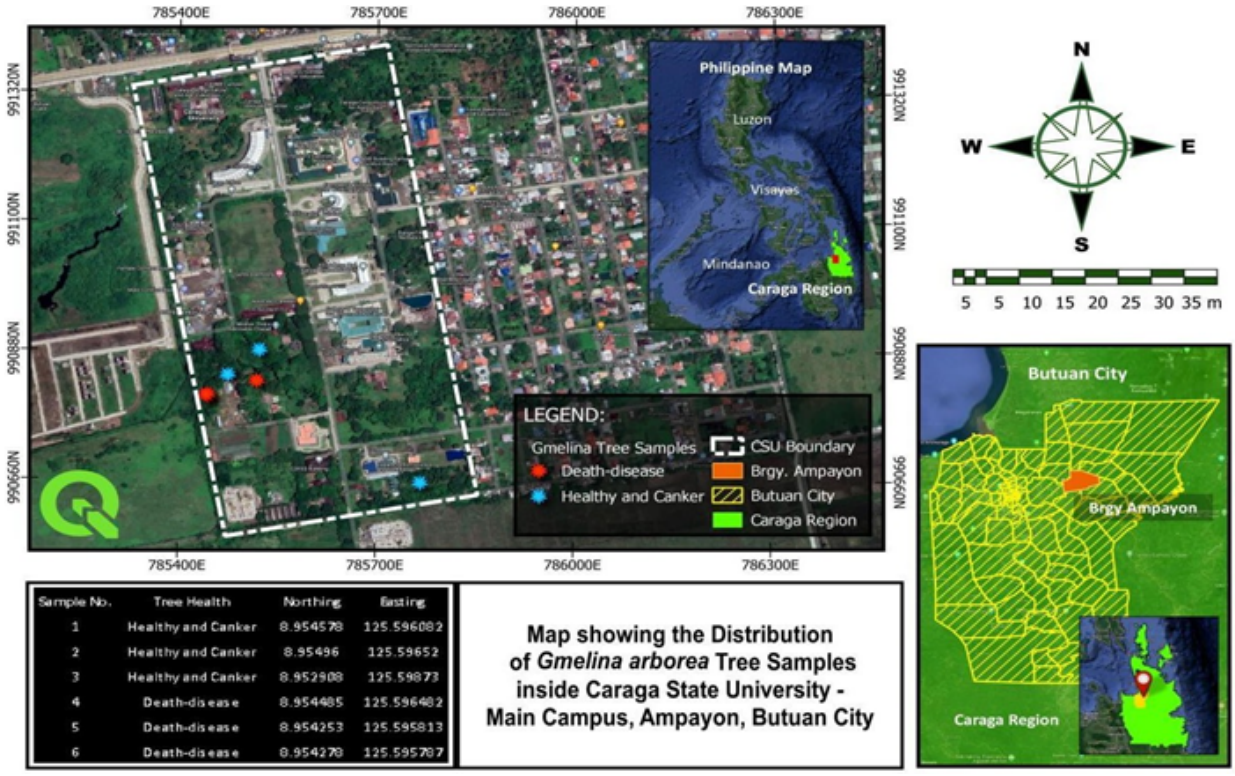

Fig. 1. Map showing the distribution of *G. arborea* tree samples inside Caraga State University.

The first three (3) *G. arborea* trees were extracted with healthy bark samples and unhealthy bark samples with canker. The bark was removed using a sharp knife and the samples were stored and sealed, during the collection plastic gloves were worn to avoid contamination (Schelle et al. 2002). Each tree acquired one (1) sample of healthy bark and one (1) sample of unhealthy bark with canker for a total of three (3) bark samples, each with three replicates of healthy bark and unhealthy bark with canker. Likewise, the other three (3) *G. arborea* trees among the six (6) trees were extracted solely with the unhealthy bark samples with death-disease, taking one (1) sample from each tree, each sample having three (3) replicates, for a total of nine (9) replicates of unhealthy bark samples with death-disease. Finally, in order to obtain precise data for the spectral analysis, nine (9) replicates of healthy bark samples were collected, as well as nine (9) replicates of unhealthy bark samples with canker and nine (9) replicates of unhealthy bark samples with death disease. After collecting the samples, they were brought to Caraga State University, College of Mathematics and Natural Sciences, and Physics Laboratory to test the difference in the wavelength absorbance of both classifications using a UV-Vis spectrometer. The data was recorded using the computer.

Table 1. Tree samples diameter at breast height (DBH)

Tree no.	Bark Samples	DBH (cm)	Class Disease severity
1	Healthy	38	#1
1	Canker		#2
2	Healthy	40	#1
2	Canker		#2
3	Healthy	24	#1
3	Canker		#2
4	Death-disease	29	#3
5	Death-disease	20	#3
6	Death-disease	24	#3

Notes: Severity #1: A healthy tree with no evidence of visible symptoms; Severity #2: Initial yellowing of the crown (evident foliar wilting), the stem may have small necrotic wounds and black exudation in places other than where pruning has occurred, and resprouting may begin. Not all symptoms are expressed; Severity #3: The tree is visibly diseased and has canker-like lesions on the bark There are canker-like lesions on the bark has signs of rot, bark exposure and bulging, and prominent oozing (Source: Salas-Rodriguez et al. 2016).

2.2.1. Collection of plant material

The researchers collected samples from identified *G. arborea* trees, focusing on healthy bark and bark affected by canker and death-disease. The visual and physical differences between healthy and unhealthy bark were documented with detailed descriptions (**Fig. 2–4**).

Fig. 2. Healthy bark (a) sample 1, (b) sample 2, and (c) sample 3 of *G. arborea* found at the study site has a similar appearance to most healthy bark of *G. arborea*. It is distinguished by a smooth and lustrous outer surface with a rich golden-brown color. The healthy bark samples show an intricate pattern of fine ridges and subtle fissures, contributing to their visual appeal.

Fig. 3. Unhealthy bark (a) sample 1, (b) sample 2 and (c) sample 3 with canker, the three samples show similar appearance that appears to be bulging, swollen and cracked.

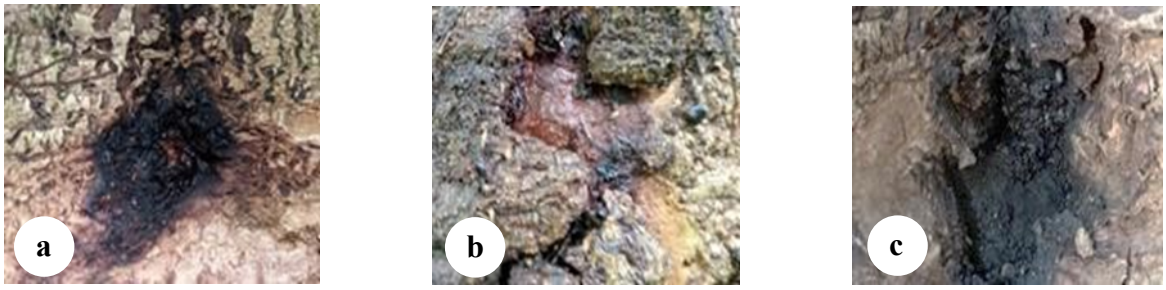

Fig. 4. The unhealthy bark (a) sample 1 and (b) sample 2 with death disease show the presence of canker and black exudation, with black exudation expanding in all areas affected, while (c) sample 3 shows mild symptoms of death disease with the presence of canker and sap, which will later turn blackish as the stress in the bark worsens.

2.2.2. Plant preparation and extraction

The specimen was brought into a laboratory to be extracted. From the sample collected, the researcher weighs 1 gram of the samples of healthy bark, canker disease, and tree-death disease, each sample has three (3) replicates. Using the mortar and pestle, the researcher crushed each sample and turned it into a fine paste, 20 ml of distilled water was added to the paste, and then it was filtered using a 125 mm diameter of Whatman filter paper number four (4) for 24 hours. The researchers ensure the safety and cleanliness of the samples to avoid contamination. After filtering the samples for 24 hours, a clean dropper was used to put enough filtered samples in a cuvette while adding 1.0 mL of distilled to dilute the solution in order to get a reading from the spectrophotometer (Dippong and Mihali 2019; Penner 2017). In a spectrophotometer machine, there are four (4) cell racks, and one (1) cell was intended for distilled water. This serves as the basis for considering the absorption of the solution in which the sample was carried. The three (3) remaining cell racks were for the filtered samples from each category (**Fig. 5**).

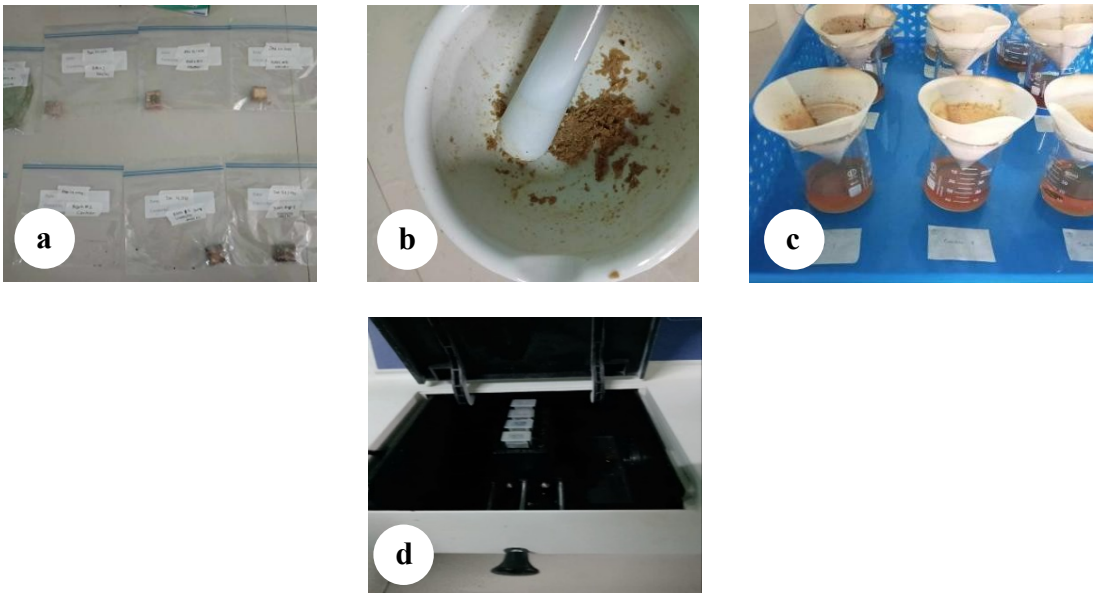

Fig. 5. (a) samples of healthy and unhealthy bark of *G. arborea* Roxb (b) samples crushed using mortar and pestle (c) all samples were filtered using a 125 mm diameter of Whatman filter paper number four (4) for 24 hours. (d) all samples were put inside the spectrophotometer machine.

2.3. Data Analysis

2.3.1. Spectral profiling UV-Vis spectrophotometer

To get the absorption of each sample of healthy bark and unhealthy bark at a specific wavelength. A UV-Vis Spectrophotometer (Spectrumlab 752s) was used, providing the absorption data of every sample at a specific wavelength. The absorbance was measured between 350–800 nm (Visible to Near Infrared spectrum), with a separation of 1nm (Fang 2021). The absorbance of each sample was manually read and calibrated. Then, the gathered data was graphed using Microsoft Excel to analyze each sample of Healthy and Unhealthy bark spectral trends. Finally, to characterize the difference in the spectral trend of the samples the average absorption of each sample with three (3) replicates was also graphed. To support the study by identifying significant differences in the spectrum, Kruskal-Wallis Tests were used involving healthy samples 1, 2 and 3 between unhealthy samples 1, 2 and 3 with canker. To determine if there is a significant difference between healthy samples and unhealthy samples with death- disease. An independent sample T-Test was used to perform the statistical analysis. Only healthy samples 1, and 2 and unhealthy samples 1 and 2 were compared since unhealthy sample 3 with death-disease only showed mild symptoms.

3. Results and Discussion

3.1. Spectral Analysis on Healthy Bark Samples

The absorption peak of healthy bark samples, as indicated in **Fig. 6** was observed with no absorbance peak. Overall findings on the absorbance of the collected average of healthy bark samples resulted in a smooth absorbance trend utilizing UV-Vis spectrophotometry. Spectra of Healthy bark samples show a comparable trend in its absorption at specific wavelengths. As seen in **Fig. 6**, there are no peak or trough formations. However, sample 1 tends to show a higher absorption on the UV region, which may indicate a difference in concentration.

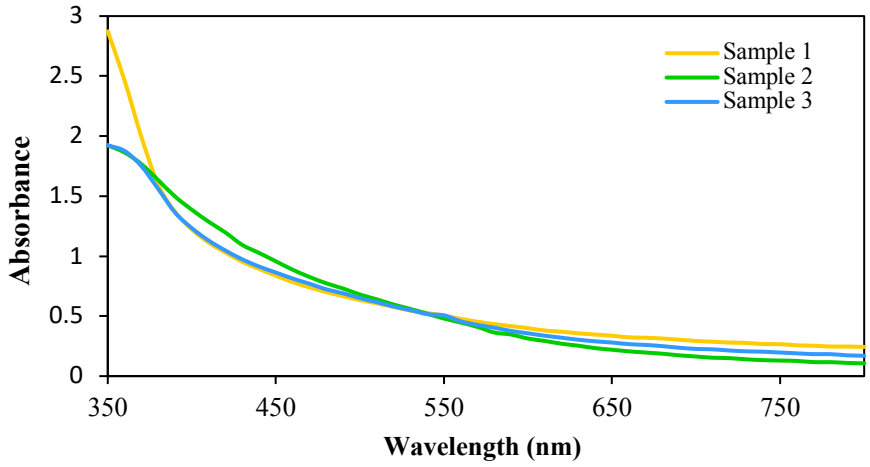

Fig. 6. UV-Vis spectra of the average absorbance of healthy bark samples of *G. arborea*.

The study of Aldabib and Edbeib (2020) indicates that according to Beer's Law, absorbance should be proportional to concentration, the sample with the highest concentration also has the highest absorbance value. The sample with the lowest concentration value also had the lowest absorption value. Thus, the effect of concentration on absorbance influences the flow of spectral

trends. This was supported by the study of Leufen et al. (2014), who found that the mechanism of this is the spectral data of healthy samples, which are different from disease samples. Different fungal diseases, as causal agents, can influence spectral data since each one triggers the production of distinct biochemical substances in response to the disease. The spectral response to pathogens can vary significantly across plant cultivars (Gold et al. 2020).

3.1.1. Spectral analysis of canker and death-disease

As shown in **Fig. 7**, samples of unhealthy bark with canker show a comparable wavelength trend with the healthy bark samples. However, sample 1 shows the presence of bumps on its wavelength trend along 400 nm to 440 nm. These bumps could mean that there is a presence of impurities or contaminants in the sample since samples 2 and 3 do not exhibit the same behavior on their absorbance trend. Since there are no specific peaks on the spectral profile of canker, it may suggest that the disease at an early stage of infection only affects the physical properties of the tree and does not directly impact and penetrate the biochemical properties of the bark, which is why it does not show any alteration on its wavelength trend It was supported by the study of Arguedas et al. (2018) that the physical properties of infected wood show lower physical properties compared to normal wood of Gmelina. Several studies show that the biochemical properties of infected parts of a plant greatly affect its spectral characteristics (Abdullah et al. 2018; Sprintsin et al. 2011). Canker wounds may form due to infections caused by pathogens, insects, or physical injuries (Verma and Meshram 2018). In general, it is impossible to detect canker clearly during the initial stages of the disease and it can be observed in cuts made above the sprouts, where depressions of the bark can be detected (Arguedas et al. 2018).

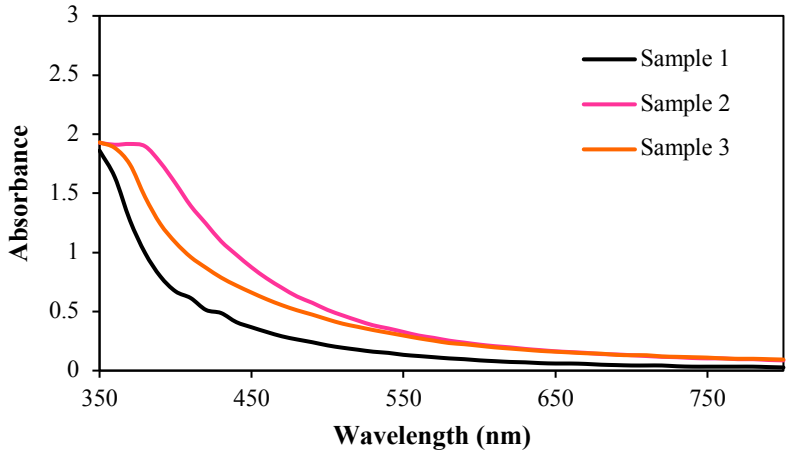

Fig. 7. UV-Vis spectra of the average absorption of unhealthy bark samples with the canker of *G. arborea*.

According to Belezaca-Pinargote et al. (2022), the wood of *G. arborea* infected by canker disease shows symptoms of necrosis caused by the pathogen. The absorption of the three unhealthy bark samples with death-disease is depicted in **Fig. 8**. Sample 1 and 2 have severe death-disease symptoms, while sample 3 has milder symptoms. Sample 1 of unhealthy bark with death-disease spectra shows a drastic decrease in absorbance between 400 nm and 420 nm, resulting in a trough in the spectral trend along 420 nm (**Fig. 8**). The result is supported by the study of Dahali et al. (2023) on the canker disease of *Eucalyptus deuterocubensis* as the extent of trees' infection was becoming severe there was also a downward trend. According to Leufen et al. (2014), the intensity

of samples with diseases is different from the normal and healthy samples because of the mechanism in its spectral data. Compared to samples 1 and 2, sample 3 shows a similar spectral trend to canker disease because it exhibits mild symptoms of death-disease (**Fig. 4c**), as opposed to the two samples, which exhibit severe symptoms. Cankers are one of the signs and symptoms seen in the early stage of death- disease on Gmelina bark (Arguedas et al. 2018). This may imply that the disease's presence and severity may affect the bark samples' spectral absorbance.

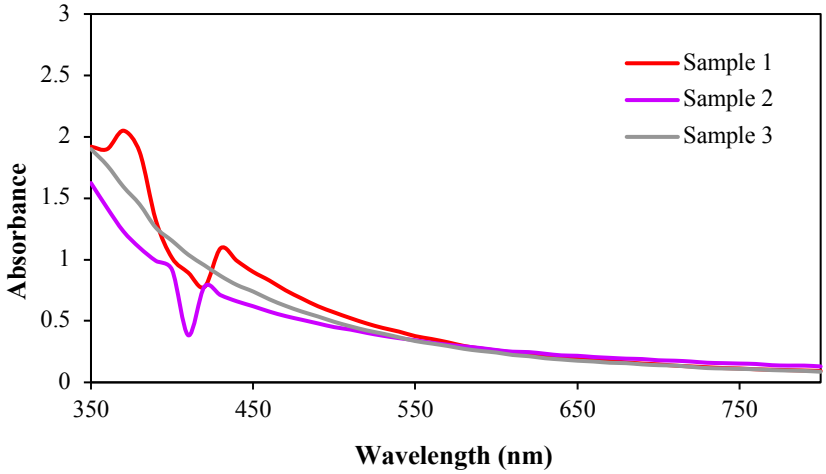

Fig. 8. UV-Vis spectra of the average absorption of unhealthy Bark samples with death-disease of *G. arborea*.

3.1.2. Comparison of the spectral characteristics of healthy and unhealthy bark samples

The spectra of the healthy bark sample will be used as a reference to determine the difference in spectral trend between healthy and unhealthy bark samples with canker. Canker is caused by the fungus *C. fimbriata* (Belezaca-Pinargote et al. 2022; Méndez-Álvarez et al. 2020), which is one of the most severe diseases attacking Gmelina and causing stem and branch canker. In **Fig. 9–11**, healthy bark samples exhibit a similar wavelength pattern. The absorption trend is smooth and does not show 350–800 nm absorption peaks. In contrast, although the spectra of unhealthy bark samples also show no absorbance peak and trough, they relatively show a lower absorbance trend than the healthy bark sample. However, no significant change in absorption peaks was observed, which can be attributed to Canker infection as shown in **Fig. 3**. This may imply that although it does not show any alteration in its spectral trend, canker does affect the absorption of the sample bark. In addition, this may also imply that canker that is not severe may only affect the physical properties and may not have a major contribution to the alteration of present biochemicals.

However, this study mostly considered reflectance spectra and not on the biochemical properties of the bark. Therefore, it is important to understand whether the biochemical properties are also affected in addition to the spectral profiling-consequently, the topic warrants further investigation. The severity of the canker disease falls under (severity criteria #2) an arbitrary five-category scale of the severity of the disease in *G. arborea* as proposed by Salas-Rodriguez et al. (2016). Statistical analysis using the Kruskal-Wallis Test was performed to support this claim further. **Table 2** shows a significant difference between Unhealthy sample 1 and all Healthy Samples. However, healthy sample 2 and unhealthy sample 3 show no significant difference in their absorption spectrum. Healthy sample 3 and unhealthy sample 2 show no significant difference. However, it is important to note the need to extend the spectra profiling of these diseases to the UV

Infrared region to confirm this claim further.

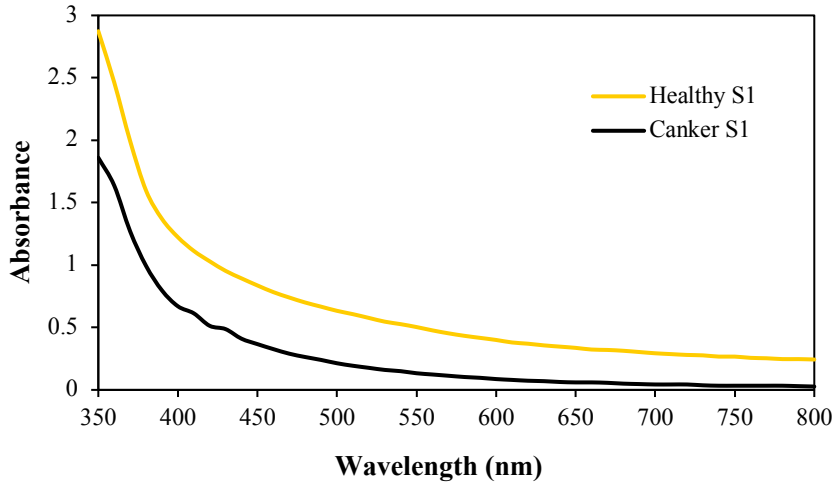

Fig. 9. The absorption spectra of the average healthy bark samples and unhealthy bark samples with canker (a) sample 1 of canker shows bumps caused by certain contaminants.

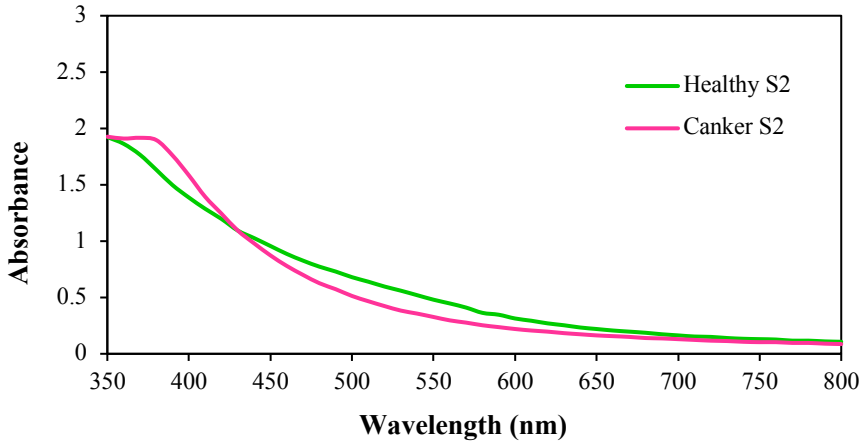

Fig. 10. The comparison of absorption spectra of the average healthy bark samples and unhealthy bark samples with canker (b) sample 2 of canker shows a decrease in its absorption.

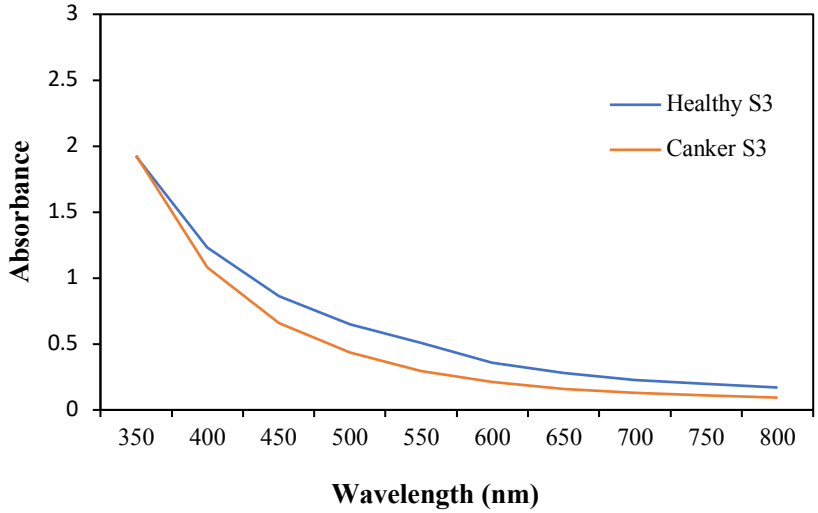

Fig. 11. The comparison of absorption spectra of the average healthy bark samples and unhealthy bark samples with canker (c) sample 3 of canker also shows a decrease in its absorption.

Table 2. Statistical analysis of absorbance

Healthy bark	Unhealthy bark	P-value
HS1	US1	0.011*
HS1	US2	0.983ns
HS1	US3	0.839ns
HS2	US1	0.002*
HS2	US2	1.000ns
HS2	US3	0.482ns
HS3	US1	0.011*
HS3	US2	0.980ns
HS3	US3	0.852ns

Notes: ** = very significant, *p*-value < 0.01; * = significant, *p*-value < 0.05; ns = non significant; *p*-value < 0.05; HS= healthy sample; UH= unhealthy sample.

3.1.3. Healthy and unhealthy bark samples with death-disease

Fig. 9–11 depicts the average absorption spectral trend for healthy and unhealthy bark samples with death-disease. Gmelina's death-disease symptoms were the existence of cankers and black exudation in the affected area (**Fig. 4**). The canker expands in all directions from the fungus point of entry, and as the symptoms worsen, black exudation appears. The affected area was distinguished from the surrounding tissue by its darker color and irregular sap secretion (Arguedas et al. 2018). Mild symptoms include the existence of canker and sap, which can eventually turn black as the pressure in the bark intensifies. *Chaetomella raphigera*, *Fusarium solani*, and *Rhizomucor variabilis* are the fungi that cause this disease. When these fungi penetrated *G. arborea*'s bark, a section turned black, identifying and classifying all symptoms related to death-disease (Arguedas et al. 2018). **Fig. 9–11** shows that the healthy bark sample's spectra display a smooth trend, with no absorption peaks and troughs at specific wavelengths.

In contrast, absorption peaks and troughs cause a significant shift in the spectral trend of unhealthy bark samples with death-disease. The presence of troughs and peaks proves an alteration in its spectral trend compared to healthy bark samples. Alteration in its spectral trend may provide useful information for determining the nature and degree of the disease or stress impacting tree bark samples. It is also possible that these alterations are the trees' response to stress or a defense mechanism. Martinelli et al. (2014) noted that when plants are exposed to pathogens, they activate defense responses, which include very complicated molecular pathways. In addition to this, he also stated that when visual symptoms appear in plants, they react to the presence of a pathogen with a physiological mechanism, such as a decrease in some biochemicals (Martinelli et al. 2014). In addition, alteration of its spectral trend may imply that it highly affects the production or the presence of specific bioactive compounds found in that particular wavelength or that there is biochemical alteration. These bioactive compounds found in the bark were flavonoids, saponins, terpenoids, and cardiac glycosides (Chugh et al. 2012).

To show statistically that there is a difference between the absorption spectrums, **Table 3** shows the independent sample T-Test of two samples 1 and 2 with death disease. **Fig. 12** shows no significant difference between healthy sample 1 and unhealthy bark with Death-Disease sample 1 based on the statistical analysis using independent sample T-Test; it may be because the spectrum of it attributes noise because the trough is not sharp. In **Fig. 13**, the statistical analysis shows a significant difference between the healthy bark and bark with death disease. Healthy sample 1 and unhealthy 2 also show a significant difference between Healthy sample 2 and unhealthy sample 1.

This can be attributed to the that the samples with death-disease already penetrated the chemical components of the bark, affecting its UV-Vis spectral properties. The observation in this study suggests a potential relationship between disease-induced chemical alterations and UV-Vis spectral properties. While this specific mechanism remains to be thoroughly investigated, related studies have reported that diseases or stress factors can alter the biochemical composition of plant tissues. For example, the study of Abdullah et al. (2018) reported that the infested bark's biochemical composition changes in its biochemical and spectral properties due to the beetle larva and blue stain fungi.

Table 3. Statistical analysis of absorbance

Healthy bark	Unhealthy bark	P-value
HS1	UH1	0.409^{ns}
HS1	UH2	0.005^{*}
HS2	UH1	0.024^{*}
HS2	UH2	$<0.001^{**}$

Note: ** = very significant, *p*-value < 0.01; * = significant, *p*-value > 0.05; ns = non significant; *p*-value < 0.05; HS= healthy sample; UH= unhealthy sample.

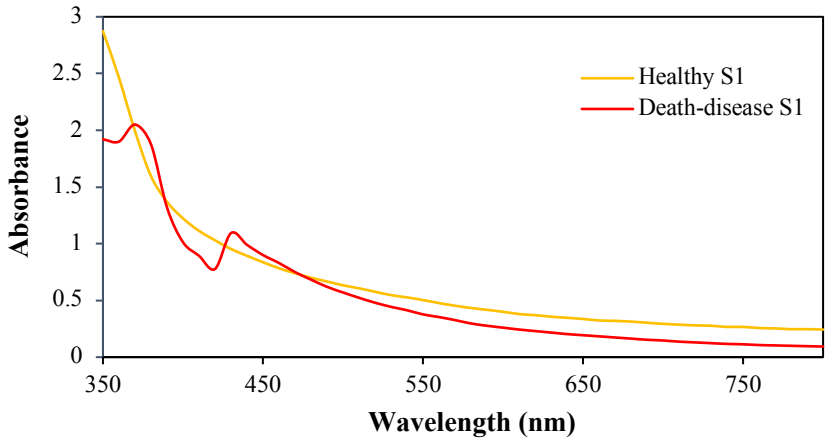

Fig. 12. Shows the comparison of average absorption spectra of Healthy bark samples and Unhealthy bark samples with death-disease (a) Sample 1 of the unhealthy bark sample shows a trough in its spectral trend along 420 nm.

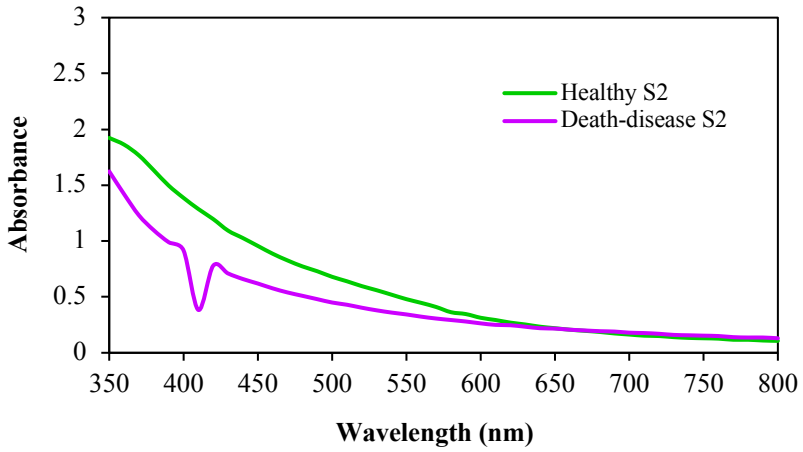

Fig. 13. The comparison of average absorption spectra of healthy bark samples and Unhealthy bark samples with death-disease (b) Sample 2 shows the presence of troughs along 410 nm.

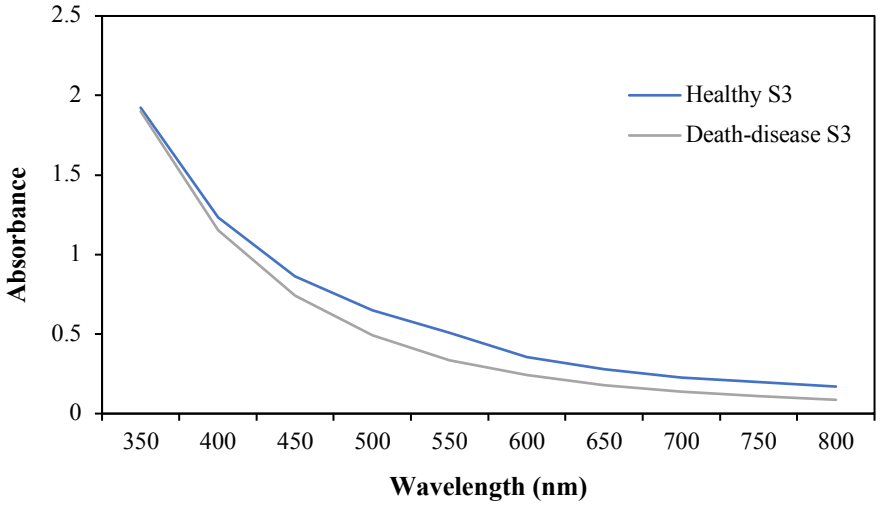

Fig. 14. Comparison of average absorption spectra of healthy bark samples and unhealthy bark samples with death-disease (c) exhibit a similar spectral trend to canker disease.

4. Conclusions

The study shows that absorbance spectra of healthy bark show a smooth behavior on its spectral trend with no presence of peaks or troughs. In contrast, absorbance spectra of bark affected by death-disease result in different spectral signatures, while bark with canker shows a relatively low absorption trend compared to healthy bark. Based on the results, the violet and blue-edge ranges in the spectrum that is in 350 nm to 450 nm were the most sensitive to the two diseases associated with the bark of *G. arborea*, but among the two diseases, it was the death-disease which is more sensitive in that specific wavelength of the spectrum. The spectral trend of death-disease shows a drastic decrease in its absorption and the presence of troughs and peaks. On the other hand, the canker shows a reduction in its absorption. The severity of disease in the bark may potentially affect the behavior of the spectral trend, this is proven in the spectral trend of death-disease. The absorbance in 350 nm to 800 nm is governed by the chemical composition, which includes the different bioactive compounds found in the bark and the physical properties of the bark, and this affects the spectral behavior of healthy and unhealthy bark. The materials and methodology of this study are encouraged to improve, such as by assessing the bioactive compounds and chemical properties of healthy bark and unhealthy bark with cankers and death-disease. However, no procedure was carried out to determine what specific bioactive compounds are affected by the alteration of the spectral trend of the spectral profile of unhealthy bark infected by canker and death-disease. Assessing the spectral signature of healthy and unhealthy bark can help monitor and implement proper disease management in *G. arborea* bark. This research serves as the preliminary investigation of spectral analysis of healthy and unhealthy bark of *G. arborea*; this provides a good starting point for discussion and further research to develop and confirm these findings.

Acknowledgments

The authors would like to express gratitude to the College of Mathematics and Natural Sciences, Department of Physics, Caraga State University, and the Center for Nanoscience and Technology for Research Entrepreneurship for their invaluable support in completing this study.

References

Abdullah, H., Darvishzadeh, R., Skidmore, A.K., Groen, T.A. and Heurich, M., 2018. European Spruce Bark Beetle (*Ips typographus*, L.) Green Attack Affects Foliar Reflectance and Biochemical Properties. *International Journal of Applied Earth Observation and Geoinformation* 64(9): 199–209. DOI: 10.1016/j.jag.2017.09.009

Abu-khalaf, N., and Salman, M. 2014. Visible/Near Infrared (VIS/NIR) Spectroscopy and Multivariate Data Analysis (MVDA) for Identification and Quantification of Olive Leaf Spot (OLS) Disease. *Palestine Technical University Research Journal* 2(1): 1–8.

Aisyah, S., Hadi, Y. S., Adly, M., Lubis, R., Maulana, M. I., Sari, K., and Hidayat, W. 2023. Influence of Puspa Wood and Coconut Trunk Combination on the Characteristics of CrossLaminated Timber Bonded with Polyurethane Adhesive. *Jurnal Sylva Lestari* 11(1): 136–162. DOI: 10.23960/jsl.v11i1.647

Aisyah, S., Haryadi, J., Maulana, M. I., Prasetia, D., Hidayat, W., Lubis, M. A. R., Kim, N. H. and Febrianto, F. 2021. Effects of Strands Pre-Treatment and Adhesive Type on the Properties of Oriented Strand Board Made from Gmelina (*Gmelina arborea*) wood. *Jurnal Sylva Lestari* 9(3): 475–487. DOI: 10.23960/jsl.v9i3.532

Aldabib, J. M., and Edbeib, M. F. 2020. The Effects of Concentration Based on the Absorbance form the Ultraviolet–Visible (UV-VIS) Spectroscopy Analysis. *International Journal of Science Letters* 2(1): 1–11. DOI: 10.38058/ijsl.633876

Alemu, K. 2015. Detection of Diseases, Identification and Diversity of Viruses. Alemu, K. (2015). Detection of Diseases, Identification and Diversity of Viruses: A Review. *Journal of Biology, Agriculture and Healthcare*. 5(1): 204–13.

Anuagasi, C. L., Onourah, J. A., and Okigbo, R. N. 2017. Fungal Pathogens Affecting Seedlings of *Gmelina arborea* Roxb and *Tectona grandis* L.F. and Effect of Three Plant Extracts. *International Journal of Agricultural Technology* 13(3): 307–330.

Arguedas, M., Rodriguez-Solis, M., Moya, R., and Berrocal, A. 2018. *Gmelina arborea* "Death Disease" in Fast-Growth Plantations: Effects of Soil and Climatic Conditions on Severity and Incidence and its Implications for Wood Quality. *Forest Systems* 27(1): e003. DOI: 10.5424/fs/2018271-12236

Belezaca-Pinargote, C. E., Solano-Apuntes, E. H., and Díaz-Navarrete, P. E. 2022. *Ceratocystis Fimbriata*: A Risk for the *Gmelina arborea* Roxb. (Melina) Forest in Ecuador. *International Journal of Health Sciences* 6(S3): 11695–11710. DOI: 10.53730/ijhs.v6nS3.8811

Belezaca-Pinargote, C., Solano-Apuntes, E., López-Tobar, R., Morales-Escobar, C. and Díaz-Navarrete, P. 2021. Presence of *Fusarium* spp. Complex in diseased trees of *Gmelina arborea* Roxb (Melina) in Ecuador. *Revista Científica Interdisciplinaria Investigación y Saberes* 11(2): 78–94.

Chugh, C. A., Mehta, S., and Dua, H. 2012. Phytochemical Screening and Evaluation of Biological Activities of Some Medicinal Plants of Phagwara, Punjab. *Asian Journal of Chemistry* 24(12): 5903–5905.

Dahali, R., Lee, S. H., Md Tahir, P., Salim, S., Hishamuddin, M. S., Che Ismail, A., Khoo, P. S., Krystofiak, T. and Antov, P. 2023. Influence of *Chrysoporthe deuterocubensis* Canker Disease on the Chemical Properties and Durability of *Eucalyptus urograndis* Against Wood Rotting Fungi and Termite Infestation. *Forests* 14(2): 350. DOI: 10.3390/f14020350

Dippong, T. and Mihali, C. 2019. UV-VIS Spectrophotometric Evaluation of the Impact of Fruit

and Wood Addition on Fruit Distillates. *Journal of Agroalimentary Processes and Technologies* 25(2): 70–74

Fang, S., Cui, R., Wang, Y., Zhao, Y., Yu, K. and Jiang, A. 2021. Application of Multiple Spectral Systems for the Tree Disease Detection: A Review. *Applied Spectroscopy Reviews* 58(2): 83–109. DOI: 10.1080/05704928.2021.1930552

Farber, C., Mahnke, M., Sanchez, L. and Kurouski, D. 2019. Advanced Spectroscopic Techniques for Plant Disease Diagnostics. A Review. *TrAC Trends in Analytical Chemistry* 118(1): 43–49. DOI: 10.1016/j.trac.2019.05.022

FMB. 2013. *Philippine Forestry Statistics Forest Management Bureau*. Department of Environment and Natural Resources, Quezon City.

Gold, K.M., Townsend, P. A., Herrmann, I. and Gevens, A. J. 2020. Investigating Potato Late Blight Physiological Differences Across Potato Cultivars with Spectroscopy and Machine Learning. *Plant Science* 295: 110316. DOI: 10.1016/j.plantsci.2019

Gudkov, S. V., Matveeva, T. A., Sarimov, R. M., Simakin, A. V., Stepanova, E. V., Moskovskiy, M. N., Dorokhov, A. S., and Izmailov, A. Y. 2023. Optical Methods for the Detection of Plant Pathogens and Diseases (Review). *AgriEngineering* 5(4): 1789–1812. DOI: 10.3390/agriengineering5040110

Hadlich, H. L., Durgante, F. M., Dos Santos, J., Higuchi, N., Chambers, J. Q. and Vicentini, A. 2018. Recognizing Amazonian Tree Species in the Field using Bark Tissues Spectra. *Forest Ecology and Management* 427(4): 296–304. DOI: 10.1016/j.foreco.2018.06.002

Hariz, T. M. R., Hadi, Y. S., Lubis, M. A. R., Maulana, M. I., Sari, R. K., and Hidayat, W. 2023. Physical and Mechanical Properties of Cross-Laminated Timber Made of a Combination of Mangium-Puspa Wood and Polyurethane Adhesive. *Jurnal Sylva Lestari* 11(1): 37–65. DOI: 10.23960/jsl.v11i1.645

Leufen, G., Noga, G., and Hunsche, M. 2014. Proximal Sensing of Plant-Pathogen Interactions in Spring Barley with Three Fluorescence Techniques. *Sensors* 14(6): 11135–11152. DOI: 10.3390/s140611135

Liaghat, S., Mansor, S., Ehsani, R., Shafri, H. Z. M., Meon, S., and Sankaran, S. 2014. Mid-Infrared Spectroscopy for Early Detection of Basal Stem Rot Disease in Oil Palm. *Computers and Electronics in Agriculture* 101: 48–54. DOI: 10.1016/j.compag.2013.12.012

Macías-Moncayo, M. L. 2019. Determination of the Causative Agent of Vascular Wilt Disease and Stem Rot of *Gmelina arborea* Roxb. in the Ecuadorian Humid Tropics. *Quevedo. UTEQ*. 62.

Martinelli, F., Scalenghe, R., Davino, S., Panno, S., Scuderi, G., Ruisi, P., Villa, P., Stroppiana, D., Boschetti, M., Goulart, L. R., Davis, C. E., and Dandekar, A. M. 2014. Advanced Methods of Plant Disease Detection. A Review. *Agronomy for Sustainable Development* 35(1): 1–25. DOI: 10.1007/s13593-014-0246-1

Méndez-Álvarez, D., de Souza Cândido, T., Couto Alfenas, A., Murillo, O., Badilla, Y. and Ferreira Alfenas, R. 2020. First Report of *Ceratocystis fimbriata* Causing Wilt on *Gmelina arborea* in Costa Rica. *Forest Pathology* 50(5): e12628. DOI: 10.1111/efp.12628

Nazarov, P. A., Baleev, D. N., Ivanova, M. I., Sokolova, L. M. and Karakozova, M. V. 2020. Infectious Plant Diseases: Etiology, Current Status, Problems and Prospects in Plant Protection. *Acta Naturae* 12(3): 46–59. DOI: 10.3 2607/actanaturae.11026

Penner, M. H. 2017. Ultraviolet, Visible, and Fluorescence Spectroscopy. Food Analysis, Springer.

Sakthivel, S., SheikAbdulla, S., Amanullah, and Safiullah. 2017. Analysis of the Extract of Barks in *Gmelina arborea* in Different Dilution and Phytochemical Examination in Ethanol Extraction. *International Journal of Pharmaceutical Science Invention* 6(9): 37–43.

Salas, A. 2015. *Determinación de la Incidencia y Severidad de la Pudricion del Tronco deGenotipos de Melina (Gmelina arborea Roxb.) en el Pacífico Sur de Costa Rica.* University of Costa Rica. Heredia, Costa Rica.

Salas-Rodríguez, A., Murillo-Gamboa, O., Murillo-Cruz, R., Ávila-Arias, C., and Mata-Granados, X. 2016. Evaluación de la Severidad de la Pudrición Del Tronco de *Gmelina arborea* (Roxb). *Revista Forestal Mesoamericana Kurú* 13(32): 1–10. DOI: 10.18845/rfmk.v0i0.2547

Sandak, J., Sandak, A. and Meder, R. 2016. Assessing Trees, Wood and Derived Products with Near Infrared Spectroscopy: Hints and Tips. *Journal of Near Infrared Spectroscopy* 24(6): 485–505. DOI: 10.1255/jnirs.12

Sankaran, S., Mishra, A., Ehsani, R., and Davis, C. 2010. A Review of Advanced Techniques for Detecting Plant Diseases. *Computers and Electronics in Agriculture* 72(1): 1–1. DOI: 10.1016/j.compag.2010.02.007

Schelle, E., Staton, I., Clarkson, P .J., Bellis, D. J. and Mcleod, C. W. 2002. Rapid Multielement Analysis of Tree Bark by EDXRF. *International Journal of Environmental and Analytical Chemistry* 82(11–12): 785–793. DOI: 10.1080/0306731021000102257

Sprintsin, M., Chen, J. M. and Czurylowicz, P. 2011. Combining Land Surface Temperature and Shortwave Infrared Reflectance for Early Detection of Mountain Pine Beetle Infestations in Western Canada. *Journal of Applied Remote Sensing* 5(1): 053566–053566. DOI: 10.1117/1.3662866

Vallesteros, A. P. 2015. *Management of Planted Trees.* A Discussion Paper for FRM 200 Advanced Forest Management College of Forestry Philippines.

Verma, R. K. and Meshram, P. B. 2018. Treatment of Standing Trees to Protect Wood Loss in Gmelina Arborea Plantations. *Indian Journal of Tropical Biodiversity* 26(1): 76–80.

Wei, X., Johnson, M. A., Langston Jr, D. B., Mehl, H. L., and Li, S. 2021. Identifying Optimal Wavelengths as Disease Signatures using Hyperspectral Sensor and Machine Learning. *Remote Sensing* 13(14): 2833. DOI: 10.3390/rs13142833